ATATÜRK ÜNİVERSİTESİ YAYINLARI
ATATURK UNIVERSITY PUBLICATIONS

Research Article *Araştırma Makalesi* DOI: 10.5281/zenodo.12566763

Numerical Investigation of The Flow Structure on Ground Surface Mounted Square Prism

Zemin Yüzeyine Monte Edilmiş Kare Prizma Üzerindeki Akış Yapısının Sayısal Olarak İncelenmesi

Onur KÜÇÜKKURT
Atatürk University, Faculty of Engineering, Mechanical Engineering Erzurum, Türkiye .

Cuma KARAKUŞ
Iskenderun Technical University, Faculty of Engineering and Natural Sciences, Mechanical Engineering. İskenderun, Türkiye.

ABSTRACT

The three-dimensional flow structure on a square prism mounted on a horizontal ground was investigated numerically using the Ansys Fluent program for Reynolds number Re = 250, 2500 and $2.5 * 10^6$, using the Standard k-ε turbulence model equations. In the study, a square prism with a large Depth Ratio (DR = 4) was used. As a result, the information was obtained about the characteristic structure of the flow around the object. For z/h= 0.05, 0.5, 0.75 and 1, the top views of the Streamlines and Turbulent kinetic energy data formed behind the ground surface-mounted square prism are shared. Streamlines and Turbulent kinetic energy side views formed in the front, top and rear flow regions of the ground surface-mounted square prism for y/D=0, 0.25, 0.5, 0.75, 1 and 1.25 are presented. On the prism surfaces, the structure of the upstream and downstream flow changed due to separation from the prism front surface and reattachment of the flow. This situation revealed the effect of the Depth Ratio on the structure of the flow topology on the object by changing the drifting flow structure and turbulent kinetic energy structure in the wake region. As the Reynolds number acting on the prism increased, the size of the vortex decreased noticeably.

Keywords: 3D Square Prism, Separated Flows, Turbulence Simulation

ÖZ

Yatay bir zemin üzerine monte edilmiş kare prizma üzerindeki üç boyutlu akış yapısı Standard k-ε türbülans modeli denklemlerinden yararlanılarak Reynolds sayısı Re = 250, 2500 ve $2.5 * 10^6$ için Ansys Fluent programı kullanılarak sayısal olarak araştırılmıştır. Çalışma da büyük derinlik oranı, (DO=4) kare prizma kullanılmıştır. Sonuç olarak cisim etrafında oluşan akışın karakteristik yapısı hakkında bilgi sahibi olunmuştur. z/h= 0, 0.5, 0.75 ve 1 için zemin yüzeye monte kare prizma arkasında oluşan Akım çizgileri, Türbülans kinetik enerji verileri üst görünüşleri paylaşılmıştır. y/D=0, 0.25, 0.5, 0.75, 1 ve 1.25 için zemin yüzeye monte kare prizma ön, üst ve arka akım bölgesinde oluşan Akım çizgileri, Türbülans kinetik enerji yan görünüşleri sunulmuştur.

Prizma yüzeyleri üzerinde, prizma ön yüzeyinden ayrılmış ve akışın yeniden bağlanması nedeniyle yukarı ve aşağı yönlü akışın yapısı değişmiştir. Bu durum iz bölgesindeki sürüklenen akış yapısını ve türbülans kinetik enerji yapısını değiştirmek vasıtasıyla derinlik oranın cisim üzerindeki akış topolojisinin yapısına etkisini ortaya koymuştur. Prizma derinlik oranın artmasıyla girdabın büyüklüğü gözle görünür oranda azalmıştır.

Anahtar kelimeler: 3 Boyutlu Kare Prizma, Akış Ayrılması, Türbülans Simülasyonu

Received/Geliş Tarihi : 13.05.2024
Accepted/Kabul Tarihi : 06.06.2024
Publication Date/Yayın Tarihi : 30.06.2024

Corresponding Author/Sorumlu Yazar:
Cuma KARAKUŞ
E-mail: cuma.karakus@iste.edu.tr

Cite this article: Küçükkurt, O., Karakuş C., (2024). Numerical Investigation of The Flow Structure On Ground Surface Mounted Square Prism, *Journal of Energy Trends*, 1(1), 21--32.

Introduction

In engineering sciences, the complex structure of flow over objects has been a subject of great curiosity in every field from the past to the present. It has been investigated in various fields of engineering, and its results have been considered in the literature. The desire to know the relationship between the fluid in motion and the object it comes into contact with has always kept the interest of researchers in this subject up to date. Numerical studies carried out using developed various software make it possible to study the pressure fields, vortex structures and vortex-induced effects of objects with complex geometries as a result of their interaction with the fluid in a shorter time and with less cost compared to experimental studies. Since real-scale investigations are very time-consuming, laborious, and costly, numerical studies provide the opportunity to reach the results in a shorter time compared to experimental studies.

If the streamlines of the flow around a body remain constant along the surface of the body and flow fields and flow separations occur on the back surface of the body, the body is aerodynamically considered to be a blunt body. Blunt bodies called 'pressure drag' are subjected to the effect of pressure drag, which is part of the total drag. Liu (2019) Blunt bodies, which are frequently used in industrial and engineering applications, are cylinders, square prisms, rectangular prisms, or spheres. The blunt body shown in Figure 1 provides information about the structure of the flow for different conditions, such as vortex intensity, vortex types, separation zone, reattachment zone, horseshoe vortex structures. In addition to the Reynolds number (Re), the shape, size, and the Depth Ratio, L/D (length/width), (DR) of the body are of great importance in the generation of these flow topologies.

In many engineering applications, the problem of flow over blunt objects such as square cylinders, circular cylinders, etc. is quite common. Flow separation, vortex shedding frequency, drag, etc. problems affecting flow are of great importance in revealing flow and aerodynamic properties due to their direct effects on engineering applications (Durhasan, 2020).

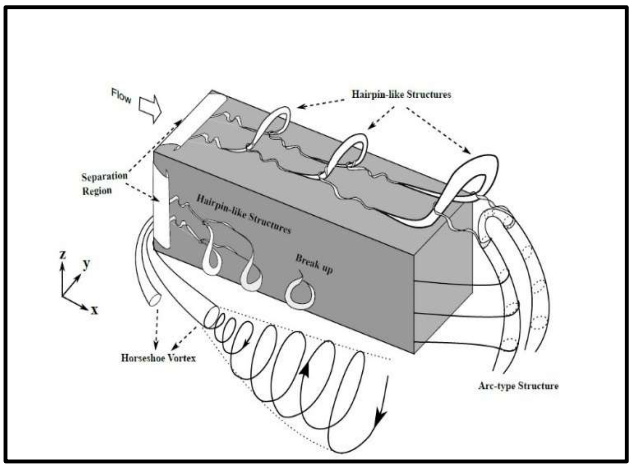

Figure 1.
Vortex structures of a long square cylinder (Zargar, 2020).

(Gao & Chow, 2005) investigated numerically two-dimensional flow over a cube. They used the Navier-Stokes Reynolds Averaged turbulence model (RANS) as the turbulence model. The aim of the study was to determine the levels of flow separation, separation and reattachment in the corner at the top of the cube. As a result, they emphasized that obtained Turbulent Kinetic Energy (TKE) values, flow separation and reattachment distances are consistent with experimental studies. Tauqeer et al. (2017) examined numerically the flow over two-dimensional square, triangular, semicircular objects using (RANS) equations. In their study, the Reynolds number was taken as Re = 10^6, while the boundary layer thickness was taken between 0.73-2.55. As a result, it is emphasized that the numerical model results are compatible with the published literature studies with high Reynolds number conducted experimentally. Korukcu (2020) analyzed the flow over a single square cylinder in two dimensions. He investigated the effect of blockage ratio (β=B/H) on the laminar continuous flow regime with the Re=40 and heat transfer. He used ANSYS CFX 14.0 in his calculations. The drag coefficient (C_d), friction coefficient (C_f), Nusselt number (Nu) on the square cylinder surfaces increased as the blockage ratio increased. Zargar et al. (2021) numerically studied the flow around a wall-mounted square prism and a square prism with a long DR for the Re=50-250. They emphasized that the vortex size decreases drastically when the DR changes. When the coefficients of friction and buoyancy are analyzed, it is found that the DR square prism is more affected than the square prism. (Wang & Lam, 2021) investigated the flow structure around a wall-mounted short square cylinder with aspect ratio (AR, H/D)=2 using experimentally Particle Image Velocimetry (PIV) and numerically Large Eddy Simulation (LES) turbulence model. In their study, they compared the experimental and numerical results of the time-averaged velocity vectors, the TKE values. As a result, they revealed that there is a difference between the PIV and the LES results in TKE

values. They stated that the Karman vortex structure is experimentally and numerically compatible. Zerrin (2021) examined numerically the structure of the flow around a square cylinder in a vertical channel for three different Reynolds numbers (Re = 100, 150, 200). Ansys Fluent software was utilized for the solution of the numerical study. She revealed that integrated heat transfer affects the flow along the channel under laminar regime conditions. (Kucukkurt & Karakus, 2024) in their study, the flow structure on the cube with AR=1 was analyzed three dimensionally and numerically. They presented information about the flow structure for Reynolds number Re=250. As a result, it is understood that has a complex structure consisting of the combination of many vortex systems depending on the Reynolds number and the shape of the cube.

Understanding the vortex dynamics of the flow around massive objects is very valuable in device design and in knowing the wind loads on architectural structures. As a result of the examination of the flow structure on the objects, it provides convenience in solving possible problems that arise or may arise in engineering applications such as high-rise buildings, bridge piers, blast furnace chimneys, truck trailers, container yards, and microchips (Goswami & Hemmati, 2023).

Flow structures formed on containers due to non-permanent wind loads in port areas may cause containers to overturn and get damaged from time to time. At the same time, it causes environmental pollution and accumulation due to the flow structure in the port areas. Therefore, it is of great importance to numerically investigate the flow structure on single- or multi-row containers and to know the flow structure. When the literature is examined, no numerical study has been found for a value of $2.5*10^6$ of the Reynolds number representing the flow on containers in port areas.

In this study, in order to simulate the flow structure on containers resembling the basic geometric shape of a square cylinder in port areas, the flow on the model with the DR = 4, which gives the ratio of container length (L) to width (D), is numerically examined. Firstly, the study was carried out for the value of Reynolds number, Re=250 depending on the square cylinder width representing very low speeds, Re=2500 representing medium speeds, and finally for the value of Reynolds number $2.5*10^6$ by taking the flow velocity as 25m/s, which is the maximum wind speed in the port area. In this study, the flow structure on a 2m width, 2m height and 8m length ground surface mounted square prism with DR= 4 is numerically calculated using Ansys Fluent program for three different Re = 250, 2500 and $2.5 * 10^6$. The flow structure in front of, on and behind the ground surface mounted square prism is analyzed.

Material and Methods

The numerical analysis flow field dimension values of the problem are shown in Figure 2. Flow analysis was performed for a square prism placed in a channel with dimensions of 11D x 5D x 34D. The width of the ground surface-mounted square prism is taken as D = 2m. Information about the views of the flow on the ground surface mounted square prism in x-y-z coordinate planes is presented also in Figure 2. The ground surface mounted square prism on the channel is assumed to be exposed to the fluid at velocity U. The velocity value was calculated for Reynolds number Re = 250, 2500 and $2.5 * 10^6$. When the literature studies are examined, it is evident that fluid air or water is used in the studies. In this study, air was used as a fluid. The ambient temperature was taken as 20 degrees Celsius. In the study, the mesh number was considered to be 2 753 431 for all Reynolds numbers. Skewness and orthogonal mesh quality value was obtained as 0.22, 0.90 respectively. Peyvandi (2024) In his study, he used the skewness value between 0.20-0.22 when defining the quality of the network structure. This value range is considered to be very good in Ansys user manual. A standard k-ε turbulence model was used to determine the flow structure.

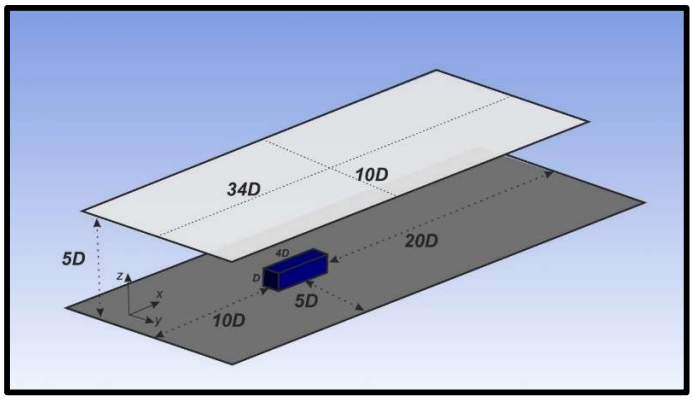

Figure 2.
Numerical analysis flow field dimensions

Standard k-ε Turbulence Model

The standard k-ε turbulence model is a common method used in practical engineering flow applications to determine both the turbulence length and time scale by solving two separate equations. It has become the preferred solution method for turbulent flow simulations by researchers because it provides economical, stable, and highly accurate results. The standard k-ε turbulence model is an approximation model that uses mathematical calculations for the turbulent kinetic energy and its dissipation rate (Rusdin, 2017).

Transport Equations for the Standard k-ε Model

This model proposed by Kolmogorov presents the equations of turbulence kinetic energy transport and its dissipation rate in Equation (1) and Equation (2). The value of the turbulence kinetic energy is determined by calculating the mean velocity gradients Chen et al. (2024)

$$\frac{\partial}{\partial t}(\rho k) + \frac{\partial}{\partial x_i}(pku_i) = \frac{\partial}{\partial x_j}\left[\left(\mu + \frac{\mu_t}{\sigma_k}\right)\frac{\partial k}{\partial x_j}\right] + G_k + G_b - \rho\varepsilon - Y_M + S_k \quad (1)$$

$$\frac{\partial}{\partial t}(\rho\varepsilon) + \frac{\partial}{\partial x_i}(p\varepsilon u_i) = \frac{\partial}{\partial x_j}\left[\left(\mu + \frac{\mu_t}{\sigma_\varepsilon}\right)\frac{\partial \varepsilon}{\partial x_j}\right] + C_{1\varepsilon}\frac{\varepsilon}{k}(G_k + C_{3\varepsilon}G_b) - C_{2\varepsilon}\rho\frac{\varepsilon^2}{k} + S_\varepsilon \quad (2)$$

Here; k is the turbulence kinetic energy, ε is the dissipation velocity, and G is the turbulence kinetic energy production due to the velocity gradients of buoyancy. σ_k and σ_ε denote the turbulence Prandtl number for k and ε, respectively. Y_M denotes the contribution of fluctuating dilatation to the overall dissipation rate in compressible turbulence. S_k and S_ε are user-defined source terms. $C_{1\varepsilon}$, $C_{2\varepsilon}$, C_μ in the equations are the turbulence Prandtl number constants. σ_k and σ_ε are the turbulence Prandtl number for k and ε, respectively. Shaheed et al. (2019)

Modeling Turbulent Viscosity

The viscosity of turbulent (eddy) flow is found by calculating μ_t (Modesti, 2020).

$$\mu_t = \rho C_\mu \frac{k^2}{\varepsilon} \quad (3)$$

Model Constants

$C_{1\varepsilon}$, $C_{2\varepsilon}$, C_μ are the turbulent flow Prandtl number constants.

$C_{1\varepsilon}$=1.44, $C_{2\varepsilon}$ =1.92, C_μ =0.09, σ_k=1, σ_ε =1.3

These default values were determined from experiments for basic turbulent flows often encountered in shear flows, such as layered flow structures and jets. They have been found to work quite well for a wide range of wall-bound and free shear flows (Ansys Fluent Theory Guide).

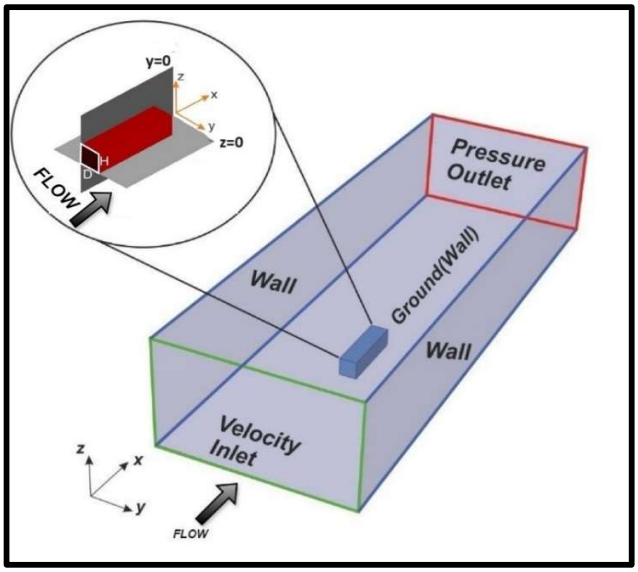

Figure 3.

Boundary conditions of the geometry in this study

The layout of the three-dimensional flow field for the ground surface-mounted square prism is shown in Figure 2 and Figure 3. The boundary conditions valid in the three-dimensional flow field on the ground surface mounted square prism are shown in Figure 3. In the selection of boundary conditions, preferences were made in accordance with the literature. Velocity inlet at the inlet and pressure outlet at the outlet ground surface and walls on the sidewalls were selected. A non-slip condition was applied to the side walls. As seen in Figure 3, the plane starting from the left side of the object is the y = 0 plane, the plane starting from the base is the z = 0 plane, and the distances y / D = 0 and z / H = 0 are the positions in the image.

Inlet:

$$u = U_\infty , T = T_\infty \quad (4)$$

Top and bottom walls:

$$u = U_\infty, v = 0, \quad T = T_\infty \quad (5)$$

Square prism walls:

$$u = 0, v = 0, \quad T = Tw \quad (6)$$

Outlet:

$$\frac{\partial u}{\partial x} = 0, \frac{\partial v}{\partial y} = 0, \frac{\partial T}{\partial x} = 0 \quad (7)$$

T_W is the temperature of the square prism wall, and T_∞ is the temperature of the incoming fluid at the boundary conditions. Reynolds number $Re = \frac{U_\infty . D}{v}$. Where U_∞ is the free flow velocity of the fluid in the channel, D is the width of the square prism mounted on the ground surface, and v is the kinematic viscosity.

In order to obtain mesh-independent solutions, experiments were carried out with different numbers of mesh structures. With the network layout created in this way, the network-independent solutions in the calculation area were defined as fine, medium, and coarse network layouts, and it was observed that the results were more consistent for the coarse network structure. (Yüce & Pulat, 2017) similarly emphasized that the method created with coarse mesh is consistent.

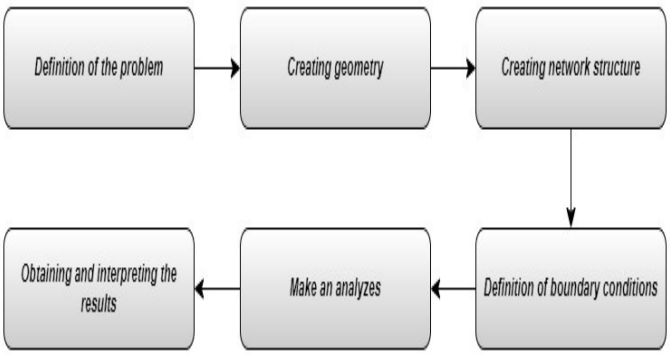

Figure 4.
Numerical analysis flow diagram

Numerical analysis flow diagram is shown Figure 4 that the flowchart of the method applied throughout the numerical study. For the numerical solutions of the three-dimensional flow field around the ground surface mounted square, the three-dimensional model was created in SolidWorks 12.0 drawing program and then imported into ANSYS. A mesh was applied to the model and boundary conditions were defined as shown in Figure 3. The Standard k-ε turbulence model was used in the numerical solution. The standard Wall Function was preferred as the wall approximation. The analysis of the model was run in FLUENT 22.1 Academic program within Erzurum Atatürk University. The results obtained are discussed in the research and discussion section.

Results

In this study, the Reynolds numbers Re = 250, 2500 and $2.5 * 10^6$ for the flow through a 2m x 2m x 8m square prism with the DR = 4 mounted on a plane are numerically investigated. In the numerical study, the flow structure is investigated for three different cases: upstream of the ground surface mounted square prism, at the free surface of the square prism and downstream of the ground surface mounted square prism. In addition, side views of the streamlines and distribution TKE images of the flow through the front, top and back surfaces of the object at y/D = 0, 0.25, 0.5, 0.75, 1 and 1.25 and top views of the streamlines and TKE images of the flow through the object at z/h = 0.05, 0.5, 0.75 and 1 are presented. The flow direction is from left to right in all images. The streamlines of the resulting vortex show negative vortices rotating clockwise and positive vortices rotating counterclockwise.

The side views of the front top and back of the ground surface mounted square prism at y/D=0, 0.25, 0.5, 0.75, 1 and 1.25 are given in Figure 5. The left column shows that the time-averaged streamlines at the front of the ground surface mounted square prism, the middle column shows that the time-averaged streamlines at the top of the ground surface mounted square prism and the right column shows that the time-averaged streamlines at the back of the ground surface mounted square prism. The horseshoe vortex is formed in front of the object at equal distance. The horseshoe vortex distances are equal for y/D=0, 0.25, 0.5, 0.75, 1 and 1.25, and the horseshoe vortex structure is 0.55D for Re = 250, 0.29D for Re = 2500, and 0.21D for Re =$2.5 * 10^6$. The results show that as the Reynolds number increases, the horseshoe vortex distance in the front region of the square prism decreases. When the images are analyzed, it is seen that the horseshoe vortex structure formed at the front of the square prism mounted on the ground surface at a distance of y/D= 0.5 for three = 250, 2500 and $2.5 * 10^6$ is more stable. Due to the onset of flow separation and the increasing pressure action on the surface of the free end of the square prism, the vertical plane midpoint moves downstream towards the surface of the square prism to form a separation bubble and reverse flow region. At the same time, shear layers can be seen between the separation bubble and the free flow region formed on the free surface of the ground surface mounted square prism. It is clearly seen that the “separation bubble” and the reverse flow region are formed due to the pressure increase along the upper surface of the prism on the offensive edge of the free end of the ground surface mounted square prism. As stated in Polat et al.

(2022) the presence of a separation bubble on the free surface of the ground surface-mounted square prism is observed due to the effect of the acceleration zone starting from the upper left edge of the body and extending along the x-axis. For Re = 250, the presence of a separation bubble and reverse flow region at y/D = 0.75 distance is clearly seen, while no stable structure is formed for other distances. For the Re = 2500 in the middle column, the presence of separation bubble and reverse flow regions for the distances y/D = 0.25, 0.5 and 0.75 is clearly seen. Depending on the height of the Reynolds number, it is seen that the vortex structure is more splayed and severe for the separation bubble formed on the free surface of the ground surface mounted square prism at Re=2500 compared to the separation bubble formed at Re=250. For Re = 250, 2500 and $2.5 * 10^6$, the separation bubble sizes formed on the ground surface mounted square prism were measured as 1.04D, 2.01D and 2.26D, respectively. Behind the free surface mounted square prism, a reverse flow region and a saddle point at some distances are observed. At Re=250, the saddle point was measured as 1.17D for y/D=0.25, 2.05D for y/D=0.5 and 1.42D for y/D=0.75. Saddle points could not be measured for distances y/D=0, 1 and 1.25. At Re=2500, this distance was measured as 0.9D for y/D=0.25, 1.6D for y/D=0.5, 1.35D for y/D=0.75 and 0.4D for y/D=1. Saddle points could not be measured for y/D=0, and 1.25 distances. At Re=$2.5 * 10^6$, the saddle points were measured as 1.06D for y/D=0.25, 1.53D for y/D=0.5 and 0.83D for y/D=0.75. Saddle points could not be measured for y/D=0, 1 and 1.25 distances. When the saddle point distances in the back region of the square prism are analyzed, it is seen that the saddle point distance decreases for almost all distances as the Reynolds number increases. Kawaii et al. (2012) stated that as the aspect ratio of the body increases, the vortex length behind the body decreases and the saddle point approaches the body. In the present study, the increase in the Reynolds number shows that the saddle point distance decreases as the aspect ratio increases. Figure 6 shows the TKE values for the ground surface mounted square prism at y/D=0, 0.25, 0.5, 0.75, 1 and 1.25 and the time-averaged velocity vectors at these distances with side views. TKE values are presented for Re=250 in the left column, Re=2500 in the middle column and Re=$2.5 * 10^6$ in the right column. When the TKE graphs are examined, it is determined that the value of the negatively rotating equilevel curves formed at the free surface trailing edge increases and is directed downwards behind the ground surface mounted square prism. However, the presence and intensity of the positively rotating vortex along the back surface of the ground surface-mounted square prism and along the downstream direction of the ground surface-mounted square prism and the plane plate junction region are observed to increase. It is observed that the maximum TKE value for Re=250, Re=2500 and $2.5 * 10^6$, occurs in the free surface escape region of the square prism at y/D=0.5 distance. The vortex distribution is clearly observed for all distances. When Figure 6 is examined, as stated in Özmen et al. (2014) the TKE value in the rear region of the ground surface mounted square prism continues to decrease from the junction point. When the time-averaged velocity vectors are analyzed, it is observed that the areas with high intensity velocity vectors on the free surface trailing edge side of the ground surface mounted square prism show areas where the velocities increase, while the areas with low intensity velocity vectors show areas where the velocities decrease or stop.

The top views of the flow through the ground surface mounted square prism for z/h = 0.05, 0.5, 0.75 and 1 distances are given in Figure 7. When the streamlines formed at z/h = 0.5 distance are examined, it is seen that the expected symmetrical structure is not formed for Re = 2500. For Re=250 and Re= $2.5 * 10^6$, it is seen that the vortex structure formed in the rear region of the ground surface mounted square prism is symmetrical and stable. For z/h=0.5 distance, the presence of one saddle point is observed at all Reynolds numbers. The saddle point at z/h=0.5 distance is 1.55D for Re=250, 0.76D for Re=2500 and 1.23D for Re= $2.5 * 10^6$. When the ground surface mounted square prism side surfaces are examined, it is seen that the vortex structure formed at z/h= 0.5 for Re= $2.5 * 10^6$ is symmetric and stable. It is understood that the vortex structure formed at z/h=0.75 for the same Reynolds number is not symmetric but still stable. For Re=250 and Re=2500, it is seen that the vortex structures formed on the side surfaces of the square prism mounted on the ground surface are not symmetrical and do not show stability.

The TKE top view passing through the square prism for z/h=0.05, 0.5, 0.75 and 1 is shown Figure 8. The TKE values of the flow through the ground surface mounted square are presented for distances z/h = 0.05, 0.5, 0.75 and 1. When the maximum TKE values are examined, it is seen that it occurs at z/h=0.5 distance for Re=250. The maximum TKE value occurred at z/h=0.75 for Re=2500 and at z/h=0.5 for Re= $2.5 * 10^6$. The TKE values show that for all Reynolds numbers at z/h=0.5 and 0.75 distance, the vortex structures on the square prism side surfaces are more stable, become sharper and the sweeping process along the square prism side plane dominates.

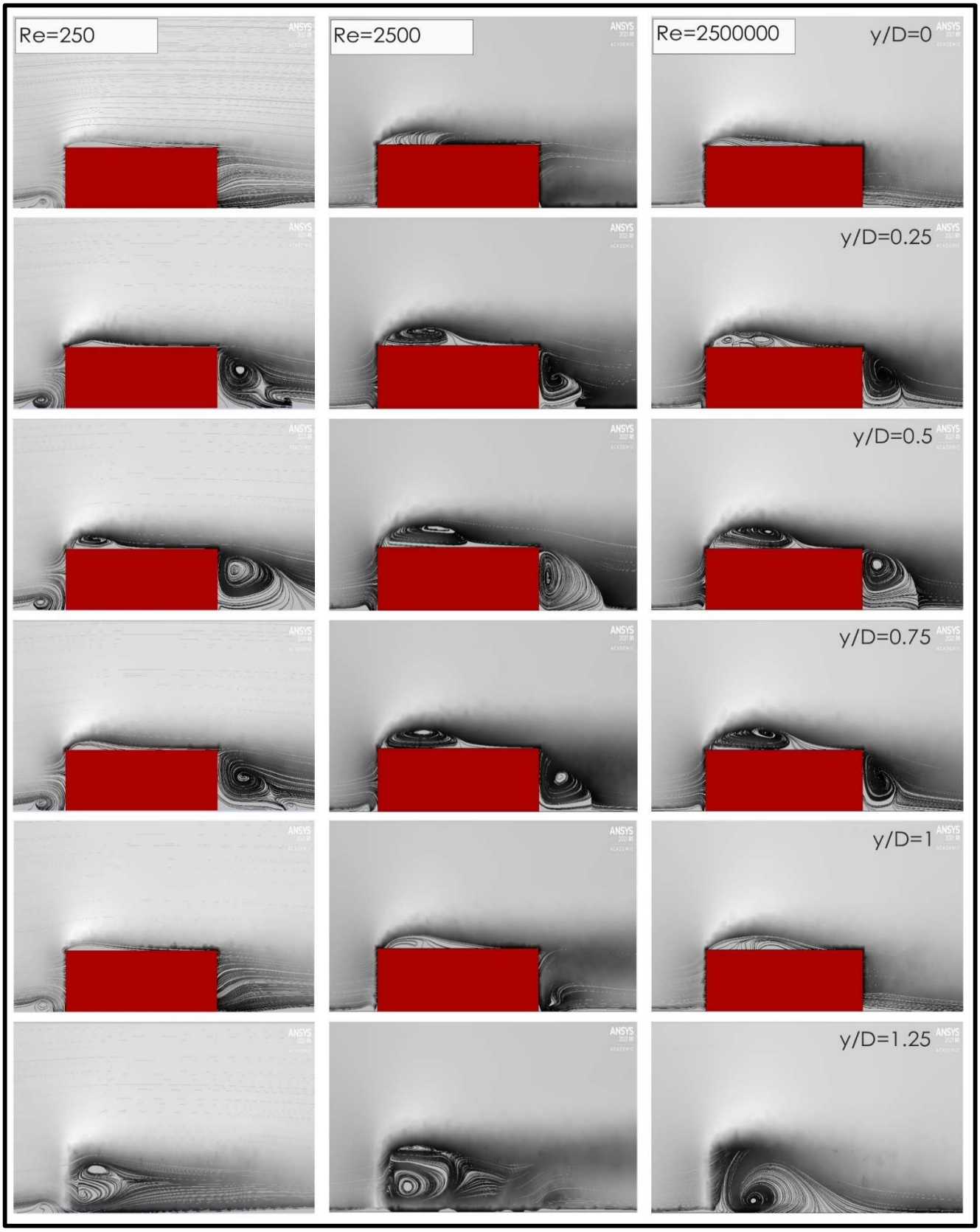

Figure 5.

Side view of the streamline formed at the front, top and back of the square prism for y/D=0, 0.25, 0.5, 0.75, 1 and 1.25

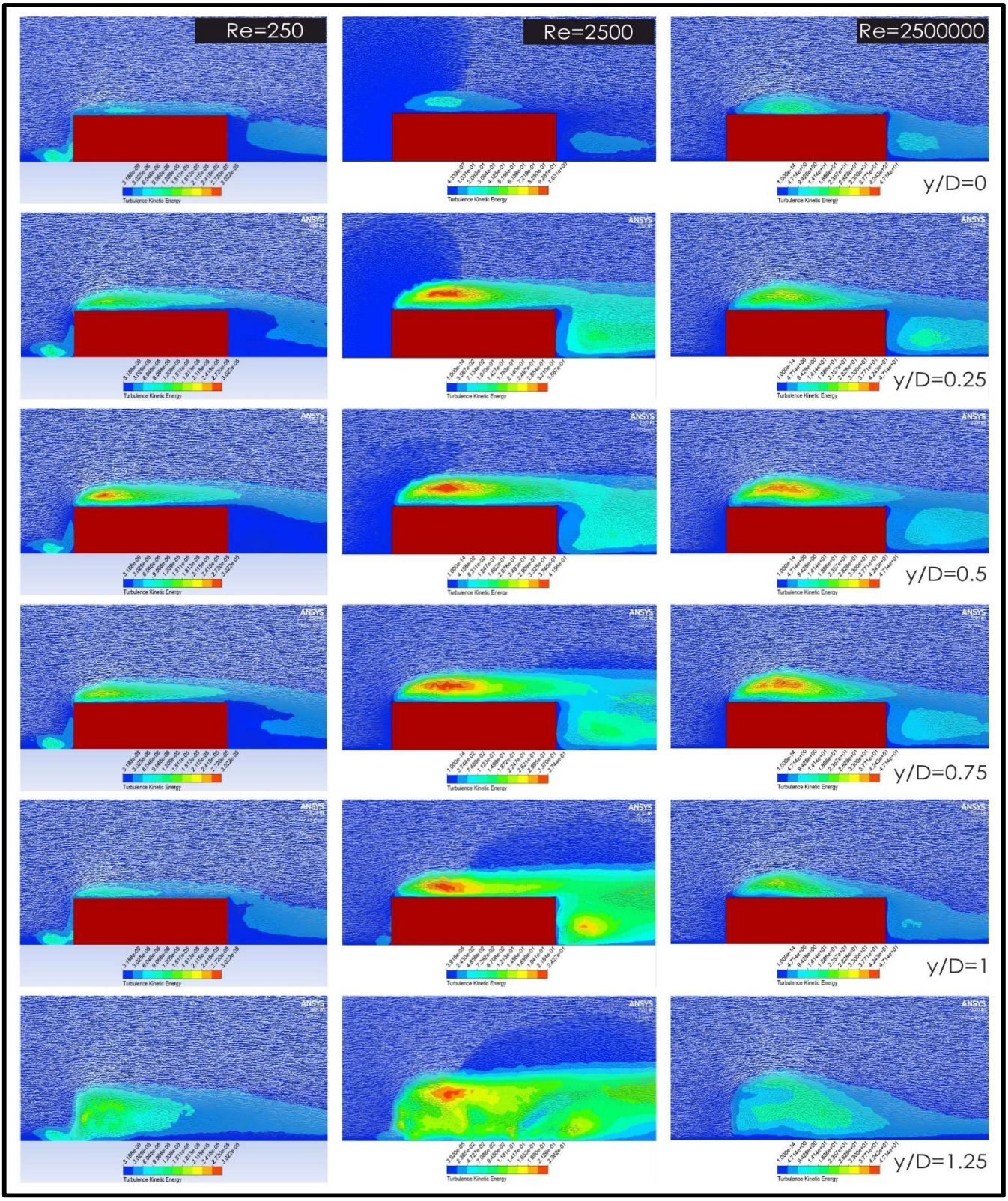

Figure 6.

Side view of Turbulence Kinetic Energy around the square prism for y/D=0, 0.25, 0.5, 0.75, 1 and 1.25

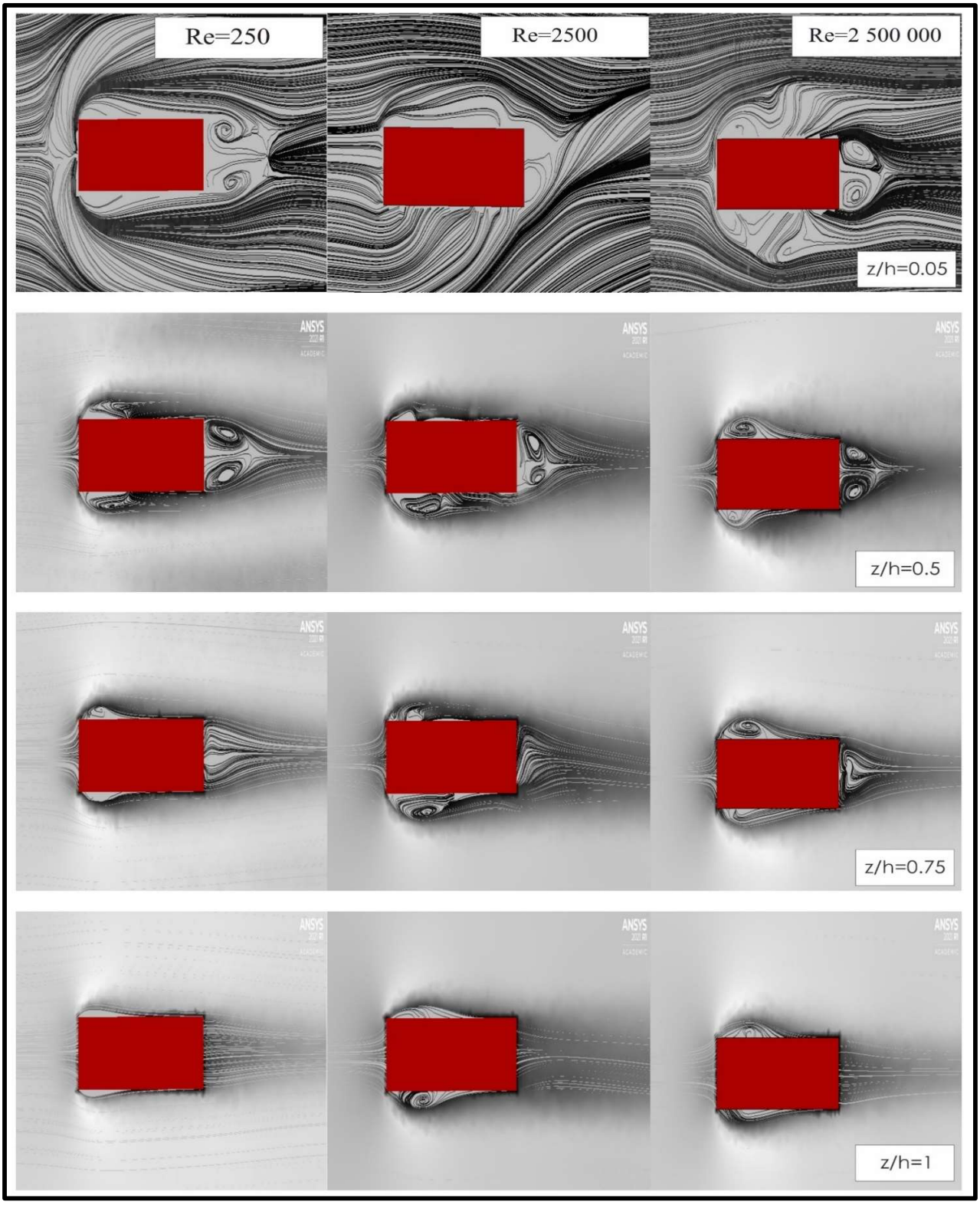

Figure 7.

Top view of the streamline passing through the square prism for z/h=0.05, 0.5, 0.75 and 1

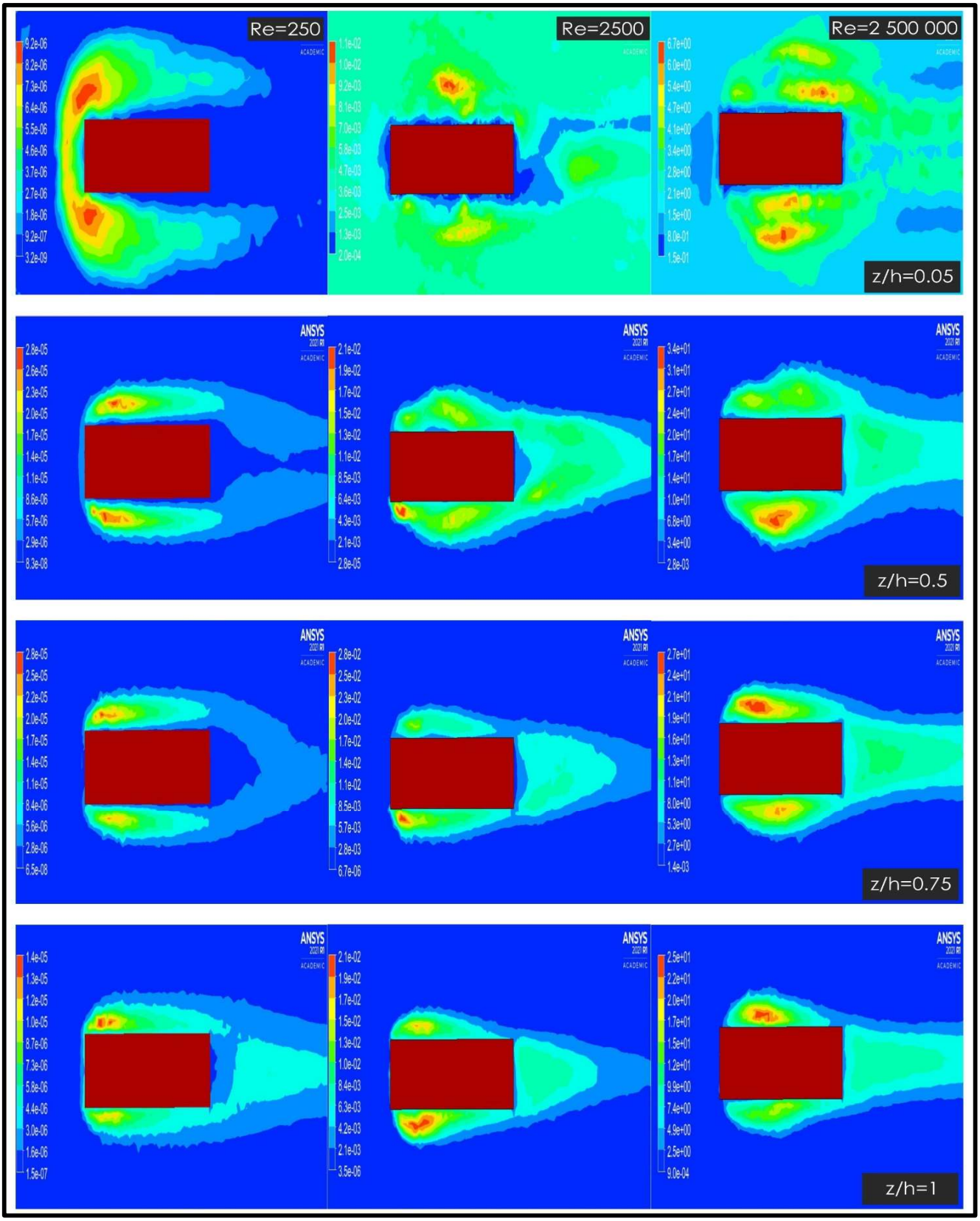

Figure 8.

Turbulent Kinetic Energy top view passing through the square prism for z/h=0.05, 0.5, 0.75 and 1

Conclusions

In this study, the flow structure over a ground surface-mounted square prism is numerically investigated using Ansys Fluent program. The ground surface mounted square prism model is D=2m wide and 8m long with the DR=4. Three different Reynolds numbers (Re=250, Re=2500, Re=$2.5 * 10^6$) are considered in this study.

It is seen that the flow in the front region of the ground surface mounted square prism forms one negative rotating vortex at the junction regions of the ground surface mounted square prism and the plane plate and this negative vortex is more stable for Re=250 and becomes unstable as the Reynolds number increases.

When the flow on the ground surface mounted square prism free surface was analyzed, a separation bubble was observed at the trailing edge of the ground surface mounted square prism free surface at a distance of y/D= 0.5 for Re=250. It is observed that the size of the separation bubble increases as the Reynolds number increases. For Reynolds numbers Re = 250, 2500 and $2.5 * 10^6$, the separation bubble sizes formed on the ground surface mounted square prism were measured as 1.04D, 2.01D and 2.26D, respectively. The flows behind the ground surface-mounted square prism reveal a complex three-dimensional structure that is affected by the horseshoe vortex structure at the base, vortex ruptures in the center region of the ground surface-mounted square prism, and flow structures on the free surface.

When the flow in the back region of the square prism mounted on the ground surface is examined, a saddle point is formed at the base of the flow region. The saddle point divides the flow into two, towards the free end of the square prism and towards the ground plane. It is seen that the saddle point distances decrease with increasing Reynolds number.

As a result, it is seen that the flow on the ground surface mounted square prism is a combination of many vortex systems and has a complex nonpermanent structure. In the back region of the ground surface mounted square prism, it is observed that a complex flow structure is formed downward from the free surface of the square prism. It was determined that the effect of the square prism the Depth Ratio (DR=4) on the formation of this complex structure was high. When evaluated in terms of engineering applications, it is thought that the complex flow structure may create undesirable situations such as structural problems.

Peer-review: *Externally peer-reviewed*

Author contributions:

O.K : Writing, Literature Search, Analysis

C.K : Supervision, Conceptualization

Financial disclosure: *This research received no external funding.*

Conflict of Interest: *The author has no conflicts of interest to declare.*

References

Ansys Fluent Theory Guide 49-50 pp.

Chen, J., & Wu, J. (2024). Numerical investigation of vortex-induced vibration of a porous-coated cylinder at subcritical Reynolds number with a combined k-ε model for porous medium. *Ocean Engineering*, 304, 117828.

Durhasan, T. (2020). Flow topology downstream of the hollow square cylinder with slots. *Ocean Engineering*, 209, 107518.

Gao, Y., & Chow, W. K. (2005). Numerical studies on air flow around a cube. *Journal of Wind Engineering and Industrial Aerodynamics*, 93(2), 115-135.

Goswami, S., & Hemmati, A. (2023). Mean wake evolution behind low aspect-ratio wall-mounted finite prisms. *International Journal of Heat and Fluid Flow*, 104, 109237.

Kawai, H., Okuda, Y., & Ohashi, M. (2012). Near wake structure behind a 3D square prism with the aspect ratio of 2.7 in a shallow boundary layer flow. *Journal Of Wind Engineering And Industrial Aerodynamics*, 104, 196-202.

Korukçu, M. Ö. (2020). Kare silindir üzerinden laminer sürekli akışta blokaj oranının ısı transferi ve akış karakteristiklerine etkisinin sayısal olarak incelenmesi. *Uludağ Üniversitesi Mühendislik Fakültesi Dergisi*, 25(1), 379-390.

Kucukkurt, O., & Karakus, C. (2024). *Zemin yüzeye monteli küp üzerindeki akış yapısının sayısal olarak incelenmesi.* AHI EVRAN International Congress on Scientific Research – IV, 578-590.

Liu R. (2019). Flow around with corner modification cross-sections, be power engineering of aircraft, [Master of thesis Nanjing University of Aeronautics and Astronautics, China].

Modesti, D. (2020). A priori tests of eddy viscosity models in square duct flow. *Theoretical and Computational Fluid Dynamics,* 34(5), 713-734.

Özmen, Y., & Kaydok, T. (2014). Kare kesitli bir yüksek bina üzerindeki türbülanslı akışın sayısal olarak incelenmesi. *Kahramanmaras Sutcu Imam University Journal of Engineering Sciences*, 17(2), 15-25.

Peyvandi, E. (2024). Numerical study of condensation and conjugated heat transfer from flow in a heat exchanger. [Master of thesis Chalmers University of Technlogy].

Polat, C., Saydam, D. B., Söyler, M., & Özalp, C. (2022). Farklı en boy oranlarına sahip karesel prizmatik cisimler etrafındaki akış

yapısının deneysel olarak incelenmesi. *Düzce Üniversitesi Bilim ve Teknoloji Dergisi,* 10(4), 1949-1959.

Rusdin, A. (2017). Computation of turbulent flow around a square block with standard and modified k-ε turbulence models. *International Journal of Automotive and Mechanical Engineering*, 14(1), 3938-3953.

Shaheed, R., Mohammadian, A., & Kheirkhah, Gildeh, H. (2019). A comparison of standard k–ε and realizable k–ε turbulence models in curved and confluent channels. *Environmental Fluid Mechanics,* 19, 543-568.

Tauqeer, M. A., Li, Z., & Ong, M. C. (2017). Numerical simulation of flow around different wall-mounted structures. *Ships and Offshore Structures,* 12(8), 1109-1116.

Yüce, B. E., & Pulat, E. (2017). *Bir ofis odasındaki termal akışın kış şartlarında sayısal olarak incelenmesi.* Teskon 2017 / Isıl Konfor Sempozyumu. 2017/080

Zargar, A. (2020). Characterization of the wake of large depth-ratio cylinders at low Reynolds numbers. [Department of Mechanical Engineering University Of Alberta Master of Science Thesis].

Zargar, A., Tarokh, A., & Hemmati, A. (2021). The steady wake of a wall-mounted rectangular prism with a large-depth-ratio at low Reynolds numbers. *Energies*, 14(12), 3579.

Zerrin, S. (2021). Kare silindir etrafında akış ve tümleşik taşınım ile ısı geçişi. *Karaelmas Fen ve Mühendislik Dergisi,* 11(2), 145-153.

Wang, F., & Lam, K. M. (2021). Experimental and numerical investigation of turbulent wake flow around wall-mounted square cylinder of aspect ratio 2. *Experimental Thermal and Fluid Science,* 123, 11032